MICROSCOPIC OBSERVATIONS OF NEEDLE AND SOFT-TISSUE SIMULANT INTERACTIONS

Alex Jahya and Sarthak Misra
MIRA – Institute of Biomedical Technology and Technical Medicine, University of Twente, The Netherlands.
email: a.jahya@utwente.nl

INTRODUCTION

One of the most common procedures employed in modern clinical practice is percutaneous needle insertion [1]. This procedure encompasses surgical operations such as prostate biopsy and brachytherapy where the accuracy of the needle placement is important. In order to correctly estimate needle tip location, physicians currently rely on their knowledge of anatomical landmarks, and on two-dimensional (2D) ultra-sound or magnetic resonance images. Nevertheless, human error, organ deformation, and physiological processes (e.g. respiration, fluid flow, etc.) may result in a wrong placement of the needle. This may lead either to complications in the biopsy procedure, or to ineffective treatment in cancer therapy [1].

A potential solution to this problem is to use a robotic device to control the placement of the needle. However, the control of this robotic device will require an accurate model of needle-tissue interaction [2]. This model can be used for planning and controlling the path of the needle during needle insertion. In order to develop this model, in situ study of needle-tissue interaction is required.

In prior work, Okamura et al. [3] have identified interaction forces during needle insertion. Furthermore, a preliminary confocal microscopic study of needle-gel interaction for manually inserted needle has been demonstrated by Misra et al [2]. However, in situ study of the gel rupture during needle insertion and the effect of gel rupture to the needle-gel interaction forces and torques is still lacking.

Thus, the aim of this study is to investigate *in situ* the gel rupture during needle insertion, and to examine how needle-gel interaction forces and torques correspond to the observations noted during gel rupture. This study involves observations of three-dimensional (3D), and time series gel rupture images that are taken during needle insertion.

METHODS

Our setup (Figure 1) is a single degree-of-freedom (DOF) planar insertion device that is mounted on a Zeiss Laser Scanning Confocal Microscope (LSCM) 510 microscope stage. In this experiment, 2% agarose gel is used as soft-tissue simulant. Moreover, the gel is doped with 100 µl fluorescin isothiocyanate (FITC). Needle and gel are visualized with differential interference contrast (DIC), epiflourescence using 488 nm line of argon laser, and 10x objective lens. DIC imaging enhances the contrast of the gel rupture, while epiflourescent imaging augments the visibility of air bubble presence in the gel.

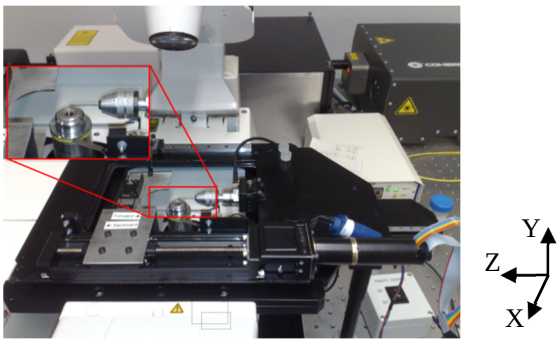

Figure 1: Experiment setup for observing needle-gel interaction under LSCM (Inset shows a self-centering, three-jaw needle chuck and the steel plate). Axis convention is shown above. Direction of insertion is in z-axis direction.

The needle (inset of Figure 1) is mounted on a 6-DOF force/torque sensor (ATI Nano-17) with force and torque resolution of 12.5 mN and 0.00625 Nmm, respectively. Solid needles of diameter Ø 1 mm with 15º, 30º, 45º and 60º bevel angles are used in the experiment. Moreover, stoppers are used to prevent movement of the gel during needle insertion. Thus, recorded forces and torques solely result from needle-gel interactions.

Force and torque data are sampled at 2000 Hz using National Instrument's LabView™ data acquisition software. The data is then averaged to reduce sampling noise. Zeiss built-in software records images at 2 s intervals for 100 cycles. A scan of one image of resolution 512 x 512 pixels will take approximately 1.7 s. Finally, gel rupture images, and their corresponding force and torque data are correlated based on the timestamp.

RESULTS AND DISCUSSION

Experimental data shows *in situ* observations of gel rupture during needle insertion. These observations are studied in relation to the force and torque data (Figure 2) and tabulated for time series analysis of the rupture (Figure 3). F_x, F_y, F_z and T_x, T_y, T_z are defined as forces along, and torques about the x-, y- and z-axis, respectively. Moreover, magnitude of the resultant torque, $||T_r||$ is defined as $||T_r|| = \sqrt{T_x^2 + T_y^2 + T_z^2}$.

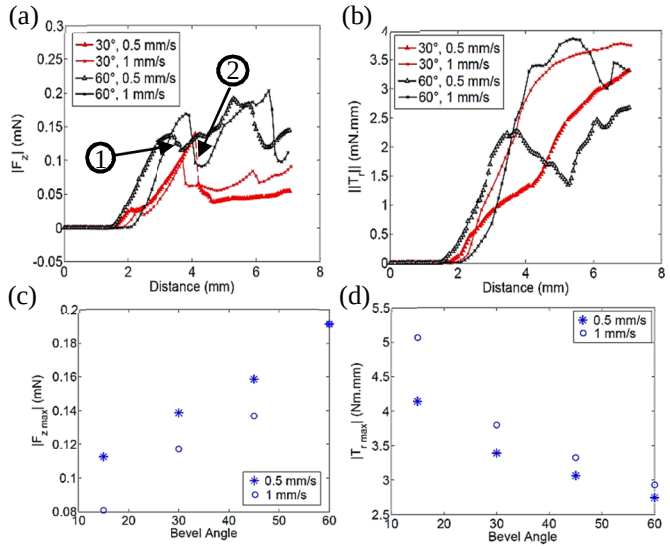

Figure 2: Plots of forces and torques for two insertion speeds, 0.5 mm/s and 1 mm/s. Numbered arrows indicate gel sudden rupture (number indicates the corresponding rupture occurrences in the images that are shown in Figure 3).

maximum $|F_z|$, and maximum $\|T_r\|$ at needle final location are defined as $|F_{z\ max}|$ and $\|T_{r\ max}\|$, respectively. T_z is zero since insertion is along the z-axis. T_y and T_x are the torques due to needle-gel interaction forces, F_x and F_y, respectively.

It is seen that an increase in the insertion speed results in stepper slope of $|F_z|$ versus displacement, and this can be noted more clearly in the plot of 60º bevel angle needle (Figure 2(a)). Similar trend can be observed in the slope of $\|T_r\|$ versus displacement (Figure 2(b)). This steeper slope might lead to the occurrence of sudden gel rupture that is characterized by a sharp drop of $|F_z|$ and $\|T_r\|$. Moreover, the increase in insertion speed also results in an earlier occurrence of sudden gel rupture.

The sudden gel rupture occurrences for 30º and 60º bevel angle needles that are inserted at 0.5 mm/s and 1 mm/s, respectively are shown with arrows in Figures 2(a) and 3. Analysis of rupture images at t = 6 s (Figure 3(a)) and t = 4 s (Figure 3(c)) shows a widening of crack bigger than the needle tip, reducing interaction/contact surface between needle tip and the gel. This most probably accounts for the sharp drop of $|F_z|$.

Moreover, $|F_{z\ max}|$ is observed to be proportional to bevel angle and inversely proportional to insertion speed. On the other hand, $\|T_{r\ max}\|$ is found to be inversely proportional to bevel angle and proportional to insertion speed. However, as needle bevel angle increases, the influence of the increase in insertion speed in $|F_{z\ max}|$ and $\|T_{r\ max}\|$ diminishes (Figure 2(c) and 2(d)). Rupture images of 60º bevel angle needle inserted at 0.5 mm/s (the second row of Figure 3) show a clearer presence of gel cutting and sliding than at 1 mm/s (the fourth row of Figure 3). In comparison, the images of 30° bevel angle needle show a comparable presence of gel cutting at both insertion speeds of 0.5 mm/s and 1 mm/s. The presence of gel cutting and sliding

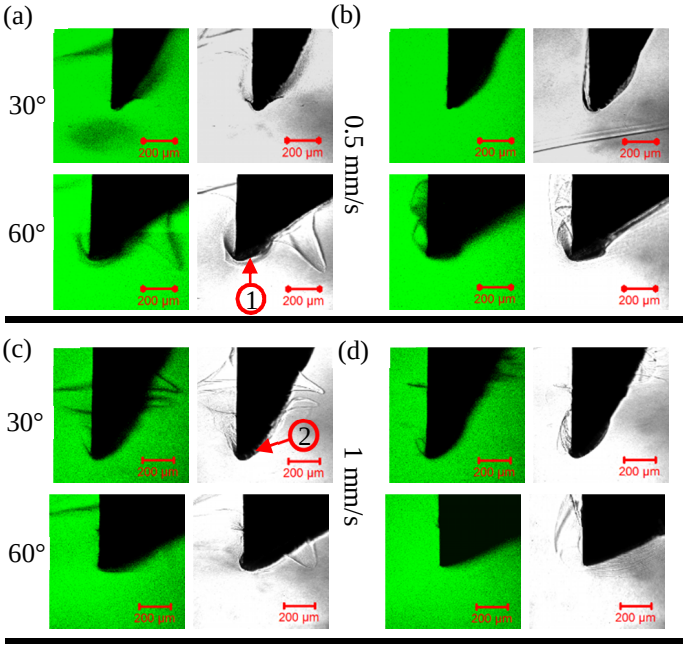

Figure 3: Epiflourescent (first and third columns) and DIC (second and third columns) images taken using the confocal microscope. Upper half rows are for 0.5 mm/s insertion speed while lower half rows are for 1 mm/s insertion speed. Timings of images are: (a) t = 6 s, (b) t = 12 s, (c) t = 4 s, (d) t = 7 s.

in 0.5 mm/s insertion of 60° bevel angle needle might account for the diminishing effect of the increase in insertion speed in $|F_{z\ max}|$ and $\|T_{r\ max}\|$. This phenomenon observed mostly in large bevel angle needle.

CONCLUSIONS

Our preliminary data have shown that it is possible to observe *in situ* gel rupture during needle insertion and to relate these rupture images to the needle-gel interaction forces and torques. Analysis of experimental data shows that the increase of insertion speed results in a sudden gel rupture. Further, experimental data shows that $|F_z|$ varies proportionally and inversely proportional with respect to bevel angle and insertion speed, respectively. On the other hand, $\|T_{r\ max}\|$ varies proportionally and inversely proportional with respect to insertion speed and bevel angle, respectively. Moreover, both, $|F_z|$ and $\|T_{r\ max}\|$ trends are shown to concur to the observations noted in gel rupture images.

ACKNOWLEDGEMENTS

The authors acknowledge the help of Auke Been in designing needle insertion device and the support from the Netherlands Organization for Scientific Research.

REFERENCES

1. DiMaio, et al. *IEEE Transactions on Robotics and Automation*, **19**(5):864-867, 2003.
2. Misra, et al., *The International Journal of Robotics Research.* **29**(13):1640-1660, 2010.
3. Okamura, et al. *IEEE Transactions on Biomedical Engineering*, **51**(10):1707-1716, 2004.